

10.5 QUANTITATIVE PRECIPITATION ESTIMATIONS FROM OPERATIONAL POLARIMETRIC RADARS FOR HYDROLOGICAL APPLICATIONS

M.-L. Segond^{1,2*}, P. Tabary² and J. Parent du Châtelet²

¹Cemagref, Anthony, France

²Météo France, Trappes, France

1. INTRODUCTION

Precipitation is the primary input to rainfall-runoff models. Meteorological radars have the potential to provide estimates of precipitation at high spatial and temporal resolution. This distributed information can be used in turn to improve our understanding of the hydrological processes of the natural system. This paper describes ongoing research with the C-band radar in Trappes, south-west of Paris, France, based on a two years polarimetric dataset to provide more accurate estimates of precipitation in an operational environment. Radar observations suffer from various types of measurement uncertainties which need to be removed before application of a rainfall rate conversion law. In this paper, we focus on possible interferences affecting the polarimetric variables. The aim is to revisit the analysis carried out by Gourley et al. (2006a), apply it to lower elevation angles and extend it to a larger number of events in order to characterise the variations of the raw polarimetric variables with azimuth. Provided these are systematic, empirical corrections procedure can then be implemented to remove these interferences prior conversion of reflectivity measurements into rainfall rate. Special emphasis is directed at differential reflectivity, for which a precision of ± 0.1 dB is necessary (Thompson, 2006). Next, two Z-R relationships for rain-rate retrieval (Testud et al (2000), Thompson (2007a)) are implemented and discussed.

Section 2 introduces the data available in this study. Sections 3 to 6 present the characterisation of the interferences affecting the polarimetric variables while section 7 proposes a correction procedure to be applied prior rainfall rate conversion. Section 8 presents the methodology and some results from two rainfall rate conversion algorithms tested in this study. Section 9 concludes with some discussion and recommendation.

2. DATA

Measurements of horizontal reflectivity (Z_H), differential reflectivity (Z_{DR}), differential phase shift (Φ_{DP}), correlation coefficient between horizontal and vertical receiving signals (ρ_{HV}) and estimated pulse-to-pulse reflectivity fluctuation (σ) from the C-band radar in Trappes are used in this investigation.

* Corresponding author address : Marie-Laure Segond, Centre météorologie radar, Météo France, 78195 Trappes, France, e-mail: marie-laure.segond@meteo.fr

These are available in polar coordinate with bin size of $240 \text{ m} \times 0.5^\circ$, except σ which is given on a 1 km^2 Cartesian grid, recorded every 15 minutes from up to 12 elevation angles for the period December 2004 - September 2006. The radar umbrella extends to a 250 km radius (1066 bins on each radial). A library of 19 events, illustrated in Tab. 1 together with the corresponding isotherm 0° altitude, served the analysis. These are constituted of data aggregated to a 24 hours time-scale and collected at 0.4, 0.8 and 1.5° elevations. For these elevations, the revisit time of the radar is 5 minutes. Focus is on the lower elevations, since the aim is to provide reasonable estimates of precipitation which are close to the ground for hydrological applications. Additionally, the 90° elevation data are used to give an estimate of the system bias.

Events	Isotherm 0° (km)	Z_{DR90° (dB) ¹	Φ_{DP90° ($^\circ$) ¹
17/12/2004	1.0	0.02	-7
24/03/2005	1.8	-0.07	-2
24/04/2005	2.1	-0.01	-2
12/05/2005	2.4	0.12	-5
13/05/2005	2.5	0.23	-3
14/05/2005	2.4	0.01	-2
06/06/2005	2.6	0.02	-3
23/06/2005	3.5	-0.04	-2
26/05/2005	3.6	0.00	-3
28/06/2005	3.3	-0.05	-2
30/06/2005	2.8	0.01	-2
04/07/2005	3.5	-0.01	-2
20/05/2006	2.0	-0.24	27
12/08/2006	2.3	-0.20	22
13/08/2006	2.1	NA	NA
29/08/2006	1.6	-0.17	21
14/09/2006	3.3	-0.17	19
15/09/2006	3.1	-0.12	19
23/09/2006	3.2	-0.14	18

Table 1 : Characteristics of selected events. NA indicates the data are not available.

¹ at 90° : mean Z_{DR} and Φ_{DP} at vertical incidence $15 < Z_H < 45$ dBZ, $\rho_{HV} > 0.97$, $1 < r < 6$ km, $n > 50\%$ for each radial

3. METHODOLOGY

The events listed in Tab. 1 are relatively spread out throughout the year with very few days available in a month therefore we focus on a daily time-step aggregation. As in Sugier (2007), the data were limited to records from light rain with Z_H values within the 20-22 dBZ range. This small interval should also ensure that the natural variability on Z_{DR} is somewhat reduced. The true mean value of Z_{DR} for this Z_H range should be about 0.2dB on average but from day to day can vary from 0.1dB - when lots of small drops are present- to 0.3dB -when the drop concentration is lower and drops are larger- (Illingworth, 2007). In addition, the criteria summarised in Tab. 2 were applied.

Range < 50 km	Local homogeneity hypothesis
Upper part of the beam < Isotherm 0° – 500m	To be in rain and avoid any bright band contamination
$\sigma > 2.5$ dB	To remove all ground-clutter pixels
Φ_{DP} around the offset $\Phi_{DP} < 10^\circ$ or $\Phi_{DP} > 240^\circ$ in 2005 $5^\circ < \Phi_{DP} < 35^\circ$ in 2006	To remove all (even slightly) attenuated pixels

Table 2 : Data selection criteria. Notice that both the 20 – 22 dBZ and the range constraints imply that all selected data have a large signal to noise ratio (SNR).

It should be noted that at vertical incidence, very few values are observed within the 20-22 dBZ range, therefore the criteria have been relaxed (See Tab. 1).

4. AZIMUTHAL VARIATIONS OF Z_{DR}

Fig. 1 displays the zero-mean daily curves of Z_{DR} . One curve corresponds to one day. “zero-mean” implies that the mean over all azimuths has been computed and subtracted to the curve). Three elevation angles are presented : 0.4°, 0.8° and 1.5°. The main masks affecting the Trappes radar are at azimuth range of [80-110°] and [280-300°], which may explain the erratic measurements observed correspondingly. Apart from this, over 360°, all curves follow a remarkably reproducible pattern, which is observed at all three elevation angles. These non symmetrical waves at 30° intervals were already pointed out by Gourley et. al (2006a) and were attributed to the 12 joints maintaining each quarter composing the radome. Sugier (2007) also reports Z_{DR} fluctuations with azimuth in relation with the structure of the radome of the UK Kent radar. It should be noted there seems to be a slight translation of the 2005 and 2006 variations, especially at azimuth range of 320-360°, where the purple curves (2006 events) are not exactly superposing the blue curves (2005 events).

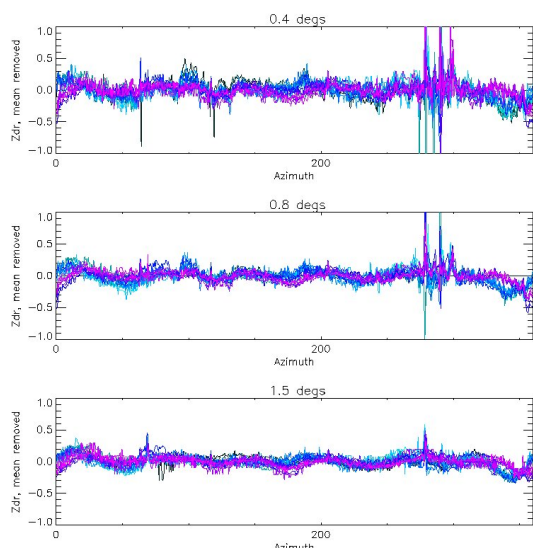


Figure 1 : Azimuthal variations of “zero-mean” Z_{DR} for all 19 events of 2005 and 2006 at elevation angles of 0.4° (top), 0.8° (middle) and 1.5° (bottom).

Mean Z_{DR} for each event at 90° elevation angles can be found in Tab. 1. This is complemented by the

mean and standard deviation of Z_{DR} for 2005 and 2006 in Tab. 3. It can be seen that except for the event of 13th May 2005, the Z_{DR} value at 90° elevation is relatively stable with 0.02 dB bias on average for all events. In 2006, the Z_{DR} value at 90° elevation seems to increase with time from -0.24 dB in May 2006 to -0.12 dB in September 2006. This temporal trend needs to be further investigated. However, once corrected for the 90° bias (column 6, 7 and 8 of Tab. 3), the Z_{DR} values in 2005 and 2006 are in agreement with mean Z_{DR} of 0.4, 0.3 and 0.2 dB \pm 0.1 at 0.4°, 0.8° and 1.5°, respectively. This is encouraging since the expected Z_{DR} corresponding to Z_H within the 20-22 dBZ range should be about 0.2 dB \pm 0.1. It should be noted that the mean Z_{DR} decreases with elevation angle. Bechini et al. (2006) demonstrated that the theoretical mean Z_{DR} decreases with altitude for elevation angle varying from 3 to 90° but this effect was purely geometric, due to the increasing radar view angle: an oblate drop seen at 90° elevation appears as circular. However this effect can be considered negligible at lower elevations, thus the decrease observed between 0.4 and 1.5° may have a microphysical explanation, e.g. increase of big drops towards the ground due to coalescence.

5. AZIMUTHAL VARIATIONS OF Φ_{DP}

A similar analysis is carried with the Φ_{DP} variations, however due to the offset change, the curves are illustrated on separate graphs at 0.8°.

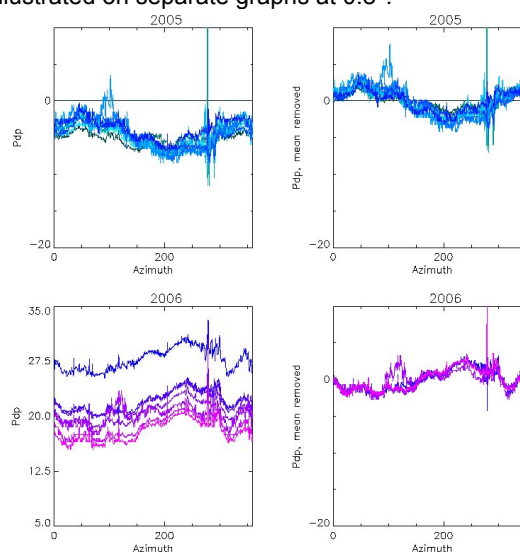


Figure 2 : Azimuthal variations of Φ_{DP} for 2005 (top) and 2006 (bottom) events at 0.8° elevation. The plots on the left side represent medians of measured Φ_{DP} . The plots on the right side represent the corresponding curves of “zero-mean” Φ_{DP} .

On the left panel of Fig. 2 are displayed the medians of Φ_{DP} , whereas on the right panel the corresponding curves are normalised by the mean. It should be noted that Φ_{DP} measurements are affected by the masks at azimuth range of [80-110°] and [280-300°]. Over 360°, a sinusoidal envelop is observed, however a different pattern is characterised in 2005 and 2006. This trend may traduce the impact of the rotary joint; and the phase

change coincides with the rotary joint being replaced in May 2006. Further in 2006, a temporal drift in the Φ_{DP} variations is observed in the case of the non-normalised medians. This offset changing in time is also highlighted in Tab. 1 with mean Φ_{DP} at 90° varying from 27° in May 2006 to 18° in September 2006. Further investigation on the system hardware of the Trappes radar is underway.

	0.4°	0.8°	1.5°	90° ⁽¹⁾	0.4°*	0.8°*	1.5°*
Mean 2005	0.44	0.34	0.26	0.02	0.42	0.32	0.24
Stdev 2005	0.12	0.12	0.10	0.08	0.14	0.13	0.12
Mean 2006	0.18	0.12	0.08	-0.17	0.39	0.32	0.26
Stdev 2006	0.35	0.25	0.19	0.12	0.08	0.04	0.04

Table 3 : Mean and standard deviation of Z_{DR} (dB) on average for 2005 and 2006 at 0.4, 0.8, 1.5 and 90° elevation angles. ⁽¹⁾ at 90° : $15 < Z_H < 45$ dBZ, $\rho_{HV} > 0.97$, $1 < r < 6$ km, $n > 50\%$ for each radial. * indicates data have been corrected of 90° bias.

6. AZIMUTHAL VARIATIONS OF ρ_{HV}

It was found that low values of ρ_{HV} (< 0.95) are occurring and these cannot be attributed to noise (recall that $20 < Z_H < 22$ dBZ and range is restricted to 50 km). In this section, we aim to quantify the number of occurrence of low ρ_{HV} values. Three classes are defined : those of $\rho_{HV} > 0.98$ (class 1), those of $\rho_{HV} > 0.90$ (class 2) and those of $\rho_{HV} > 0.70$ (class 3). Azimuthal variations of these classes are plotted for each event and the median curves for each class at 0.4 and 1.5° elevation angles are presented in red in Fig. 3.

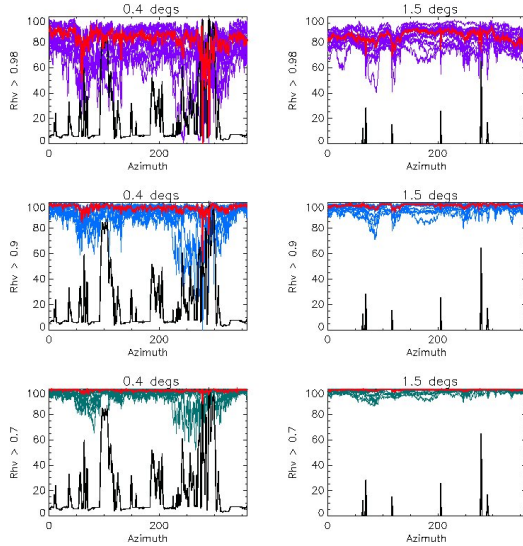


Figure 3 : Occurrence of ρ_{HV} as a function of azimuth at elevation angle of 0.4° and 1.5° . For each event, the purple curves represent the percentage of ρ_{HV} above 0.98, the blue curves represent the percentage of ρ_{HV} above 0.9 and the green curves represent the percentage of ρ_{HV} above 0.7. The median of all events is represented in red. The mask percentage is represented in black.

In addition, the percentage of mask, retrieved from numerical simulations and analysis of long-term accumulation, is also included. From Fig. 3, it can be seen that a decrease of ρ_{HV} usually corresponds to the position of the masks, and that higher values are recorded with increasing elevation angles as the impact of the masked areas is less. This behaviour is probably due to reflectivity gradients within the resolution volume, a phenomenon that has recently been formalized by Ryzhkov (2007). However, imposing a threshold on ρ_{HV} (> 0.96) did not improve the reproducibility of the Z_{DR} and Φ_{DP} curves and therefore we do not recommend implementing it at this stage.

7. PROPOSED CORRECTION PROCEDURE ON Z_{DR} AND Φ_{DP}

Hence systematic variations of Z_{DR} and Φ_{DP} with azimuth were observed. Correction procedures to remove them are proposed in this section.

7.1 Z_{DR}

The measured differential reflectivity Z_{DR}^m , can be seen as the sum of the expected ("true") differential reflectivity Z_{DR}^T , a global error term, ΔZ_{DR_0} , due to the hardware calibration of the radar and an additional azimuthal bias $\Delta Z_{DR_{AZ}}(AZ)$:

$$Z_{DR}^m = Z_{DR}^T + \Delta Z_{DR_0} + \Delta Z_{DR_{AZ}}(AZ) \quad (1)$$

At vertical incidence, given that all raindrops appear spherical, the expected Z_{DR}^T is 0 dB. In addition, on average for all azimuths, at 90° elevation, we assume that we can neglect the azimuthal bias $\Delta Z_{DR_{AZ}}(AZ)$. Therefore, for each event, ΔZ_{DR_0} is the bias deduced from measurements at 90° elevation.

At horizontal incidence, for Z_H within 20-22 dBZ, the expected $Z_{DR}^T = 0.2$ dB (Illingworth, 2007) consequently, for each event the azimuthal bias can be written as:

$$\Delta Z_{DR_{AZ}}(AZ) = Z_{DR}^{m_{20-22}} - 0.2 - \Delta Z_{DR_0} \quad (2)$$

where $Z_{DR}^{m_{20-22}}$ represent the measured differential reflectivity within the 20-22 dBZ range. Equation (2) is derived for each event and the median of the $\Delta Z_{DR_{AZ}}$ curves for 2005 and 2006 separately, is taken as the azimuthal variation correction curve to be applied subsequently to all range of Z_H in rain.

Hence for all range of Z_H in rain, the expected

Z_{DR} can be obtained as follow:

$$\Delta Z_{DR}^T = Z_{DR}^m - \Delta Z_{DR_0} - \Delta Z_{DR_{AZ}}(AZ) \quad (3)$$

It should be noted that ΔZ_{DR_0} is constant for each azimuth and elevation angle but can vary from day to day. In this case, we set a value of 0.02 dB in 2005 but implement a different ΔZ_{DR_0} for each event in 2006. $\Delta Z_{DR_{AZ}}(AZ)$ is dependent on both the azimuth and elevation angles and one curve can be derived for 2005 and 2006, separately.

7.2 Φ_{DP}

Computing and monitoring the azimuthal variations of Φ_{DP} may not be necessary if the Φ_{DP} profiles are normalized dynamically, i.e. the Φ_{DP} value at the first available gates in rain is subtracted to the remaining gates of the profile. However, we have noticed after three years of operations that the Φ_{DP} offset was a very good tracer of any change in the radar system. Hence it is important, from an operational point of view, to monitor it over time and trigger an alarm in case of a sudden change (see for instance the drift in 2006, Fig. 2).

The Φ_{DP} profiles can also be normalized using a static, yet azimuth and elevation dependent, Φ_{DP0} curve. The advantage over the dynamic approach is that it is much more robust with respect to the presence of misclassified clutter pixels. Indeed in that case, the estimation of the Φ_{DP} in the 'first available gates' may be erroneous, which would corrupt the entire ray. The dynamic approach may also fail in the case of attenuating rain occurring in the close-range ground-clutter area around the radar. In that case, attenuation does indeed occur (with differential phase rotation) over the ground-clutter area but the measurements are contaminated by ground-clutter and are thus useless. The first available gates are already attenuated but the amount of attenuation is not accounted for.

Once the Φ_{DP} profiles are normalised, the Path Integrated Attenuation (PIA in dB) is computed according to (Gourley et al., 2006b):

$$PIA = \gamma \times \Phi_{DP}^N \quad (4)$$

where γ represents a coefficient depending on temperature, hydrometeor type and Particle Size Distribution. Φ_{DP}^N represents the normalised Φ_{DP} for each bin. This in turn serves to correct Z_H measurements affected by attenuation.

8. DERIVING PRECIPITATION ESTIMATES

The correction procedures presented above were applied to the data. In this section, the aim is to test two polarimetric rainfall conversion algorithms. Since the 1.5° elevation data are smoother and less affected by the masked areas, the algorithm is applied first at this elevation angle. Besides, it was concluded that the 2006 data were also affected by a system bias. Therefore we restrict the analysis to the 2005 events.

8.1 The Z-ZDR approach (Thompson, 2007a)

Methodology

The algorithm makes use of Z_H and Z_{DR} to derive the rainfall rate and this section is mostly adapted from Thompson (2007a). The algorithm can be applied in moderate rain ($Z_H > 20$ dBZ) in case where there is no attenuation and no partial beam blocking. The algorithm assumes a normalised gamma distribution (Illingworth and Johnson, 1999) to represent the drop size distribution. This distribution has three parameters: the normalised drop concentration N_w ($m^{-3}mm^{-1}$), the shape parameter μ and the median drop parameter D_0 (mm). Consequently, the reflectivity (Z , mm^6m^{-3})-rainfall rate (R , mmh^{-1}) relationship $Z = aR^{1.5}$ can be established, where a is proportional to $1/\sqrt{N_w}$, assuming a constant shape parameter, μ . The aim is to vary N_w via a scaling factor T (in dBZ) according to (5), to find a , which best fits the data over a certain domain.

$$N_w = 8000 \left(10^{\left(\frac{T-42.34}{10} \right)} \right) \quad (5)$$

Using numerical simulations, the theoretical curve of constant N_w is approximated using the third-order polynomial (Thompson, 2007b):

$$Z_H (dBZ) = -3.1317(\log Z_{DR})^3 + 6.4566(\log Z_{DR})^2 + 32.3217(\log Z_{DR}) + T \quad (6)$$

applicable at C-band.

In the (Z_H, Z_{DR}) space, the observed values of Z_H (dBZ) and Z_{DR} (dB) are plotted together with the theoretical curve (6). Assuming that we can neglect the errors in the Z_H direction, the value of T retained is the one that minimises the root mean square error (RMS) in the Z_{DR} direction.

Application

In this investigation, we define a 100 x 100 km² radar window centred at the radar where we consider regularly spaced 5 x 5 km² square in which the methodology is applied. At this distance, we assume that the 1.5° data can provide reasonable estimates of precipitation at the ground. This is illustrated on Fig. 4 for the event of 4th July 2005. One can see that equation (6) fits well the observed data for 4 particular domains. This corresponds to N_w of 2200 (top) and 3900 (bottom) $m^{-3}mm^{-1}$ and a of 264 and 198, respectively. The algorithm is now implemented on the 2005 database to derive rainfall rate maps.

Some issues regarding the Thompson algorithm are already identified and would need to be taken into

account when implementing the methodology at an operational level:

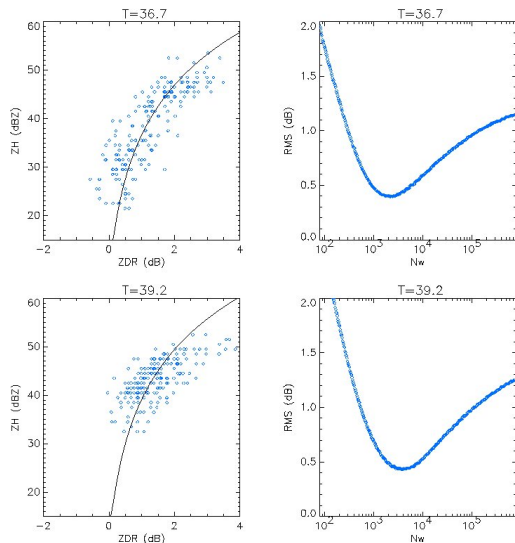


Figure 4 : Plots of observed Z_H (dBZ) vs Z_{DR} (dB) and the event of 4th July 2005 at 00h00 (left) on two successive 5 by 5 km² domain. The line of best fit is illustrated in black. T has the unit of dBZ. The corresponding curve showing the method of estimating the optimal N_w is shown on the right panel.

- The scale-dependency of the parameter « a » with the integration domain needs to be assessed.
- There may be some discontinuity in the rainfall rate map arising with the integration domain.
- Some alternative algorithms should be proposed in case of attenuation, bright band, snow and low Z_H . For $Z_H < 20$ dBZ, although the corresponding rainfall rate is low (< 0.2 mm/hr), this trace rainfall accumulated over a certain period may be significant.

8.2 ZPHI algorithm (Testud et al., 2000)

The ZPHI algorithm (Testud et al., 2000) is applied on the same 2005 dataset. The ZPHI method relies entirely on horizontal reflectivity (Z_H) and differential phase (Φ_{DP}). It does not make use of the Z_{DR} parameter. ZPHI is complementary to the so-called Z- Z_{DR} approach in the sense that it is triggered only in case of attenuation. A minimum of 6° Φ_{DP} phase rotation is indeed required to perform attenuation adjustment and N_w adjustment. In case of too low phase rotation, then a default climatological Z-R relationship is used $Z = 282.R^{1.66}$. Previous work on the evaluation of ZPHI (Szalinska et al. 2005) showed an excellent ability to correct for attenuation caused by rain but slightly disappointing results regarding N_w adjustment. Recent analyses (Testud, 2007) using disdrometer-based statistics of N_w indicated that the radome induces Z_H azimuthal variations, very similar to those on Z_{DR} . The amplitude of those Z_H perturbations is ± 0.5 dB, which is enough to corrupt the N_w estimation. Similarly to what was done for Z_{DR} , an empirical correction curve for Z_H was established and the

2005 episodes are reanalyzed using that correction.

9. CONCLUSIONS

Based on 19 events, taking over the December 2004-September 2006 period, an analysis on the azimuthal variations of the polarimetric variables was undertaken and the main conclusions are:

There is a repetitivity of Z_{DR} with azimuth, which can be attributed to the joints maintaining the radome and confirms the findings of Gourley et al. (2006a). Although similar variations were observed across all events, it was found that the Z_{DR} variations for the 2006 events were not superposing exactly the 2005 ones, thus we suggest to treat them separately. In addition, Z_{DR} was affected by a constant system bias, which can be deduced from the mean Z_{DR} measured at vertical incidence. The Z_{DR} computed at vertical incidence was relatively small and stable in 2005 with mean value (and standard deviation) across all events of 0.02 dB (0.08 dB). In 2006, the mean Z_{DR} seemed to increase with time from -0.24 dB to -0.12 dB, with a mean value (and standard deviation) of -0.17 dB (0.04 dB). We propose a procedure such that the expected differential reflectivity, can be corrected from the azimuthal bias and the system bias according to Equation (3). The system bias is given by the 90° offset and a single value could be taken for 2005 whereas it varies on a daily basis in 2006.

Regarding Φ_{DP} , results showed an azimuthal variation and this was attributed to the rotary joint (Gourley, et al. 2006a). The analysis highlighted the phase shift occurring in 2006 coinciding with the rotary joint being changed. Two normalization procedures were discussed : one based on a static Φ_{DP0} curve and the other one based on a dynamic estimation of the initial Φ_{DP} on each ray. Beyond the discussion on the most suited procedure for operational applications, it appears important – after three years of operations, to monitor over time the differential phase offset as Φ_{DP} , which was found to be a very good tracer of any change in the system hardware.

It is believed that even not optimal, the recommendations made above improve satisfactorily the accuracy of the polarimetric variables for further processing. Next, two complementary techniques (Thompson, 2007a; Testud et al. 2000) to retrieve precipitation amount were implemented based on the 2005 events at 1.5° elevation angle. Comparisons of the two algorithms will be reported subsequently. It is shown that both algorithms are extremely sensitive to the accuracy of the Z_{DR} calibration on the one hand (Thompson, 2007a) and of the Z_H calibration (Testud et al. 2000) on the other hand. The main advantage of radar data is that it allows for a spatial representation of the rainfall field. The prospects for improved precipitation estimates can be seen in the use of polarisation radars. However, depending of the rainfall rate conversion law applied the spatial structure of the rainfall changes. The importance of

this needs to be assessed jointly with continuous distributed rainfall-runoff procedures.

Acknowledgement

This work is carried out within the Programme Aramis Nouvelles Technologie en Hydrometeorologie Extension et Renouvellement (PANTHERE) project supported by Meteo-France, the French "Ministere de L'Ecologie et du Developpement Durable," the "European Regional Development Fund (ERDF)" of the European Union, and CEMAGREF. We would like to thank A. J. Illingworth, R. J. Thompson and J. Sugier for valuable discussion. In addition, we would like to acknowledge A. Le Hénaff and K. Dokhac for their help in the implementation of the codes.

Thompson, R. J., 2007a: Rainfall estimation using polarimetric weather radar, PhD thesis, The University of Reading, 183 pp.

Thompson, R. J., 2007b: Personal communication

REFERENCES

Bechini, R., Cremonini, R., Gorgucci, E. and Baldini, L., 2006: Dual-pol radar calibration and correction of the bias introduced by non uniform random wetting, Proceedings of the Fourth European Conference on Radar in Meteorology and Hydrology, Barcelona, Spain, pp 593-596.

Gourley, J., Tabary, P. and Parent-du-Châtelet, J., 2006a: Data Quality of the Meteo-France C-Band Polarimetric Radar, *Journal of Atmospheric and Oceanic Technology*, **23**: 1340-1356.

Gourley, JJ, P. Tabary, J. Parent-du-Chatelet, 2006b: Empirical estimation of attenuation from differential propagation phase measurements at C-band, *J. Appl. Meteor.*, **46**, No. 3, 306 – 317.

Illingworth, A. J. and Johnson, M. P., 1999: The role of raindrop shape and size spectra in deriving rainfall rates using polarisation radar. Preprints, *29th Int. Conf. On Radar Meteorology*, Montreal, Quebec, Canada, 301-304.

Illingworth, A. J., 2007: personal communication, February 2007.

Ryzhkov, A., 2007 : The impact of beam broadening on the quality of radar polarimetric data, *J. Atmos. Oceanic Technol.*, **24**, 729 – 744.

Sugier, J., 2007: Effects of radome and near-radome interference on differential reflectivity. UK Met. Office technical report, March 2007.

Szalinska, W., P. Tabary and H. Andrieu, 2005: Conditional evaluation of conventional vs. polarimetric QPE at C-band, Preprints, *31st Int. Conf. On Radar Meteorology*, Albuquerque, USA.

Testud J., Le Bouar, E., Obligis, E. and Ali-Mehenni, M., 2000: The rain profiling algorithm applied to polarimetric weather radar. *Journal of Atmospheric and Oceanic Technology*, **17**: 332-356.

Testud, J., 2007: personal communication, March 2007.